Kerr detection of acoustic spin transport in GaAs (110) quantum wells

A. Hernández-Mínguez, K. Biermann, S. Lazi, R. Hey, and P. V. Santos

Citation: Applied Physics Letters **97**, 242110 (2010); doi: 10.1063/1.3524218
View online: http://dx.doi.org/10.1063/1.3524218
View Table of Contents: http://scitation.aip.org/content/aip/journal/apl/97/24?ver=pdfcov
Published by the AIP Publishing

Kerr detection of acoustic spin transport in GaAs (110) quantum wells

A. Hernández-Mínguez,[a] K. Biermann, S. Lazić, R. Hey, and P. V. Santos
Paul-Drude-Institut für Festkörperelektronik, Hausvogteiplatz 5-7, 10117 Berlin, Germany

(Received 29 September 2010; accepted 12 November 2010; published online 16 December 2010)

Time-resolved Kerr reflectometry (TRKR) is used to investigate the long-range transport of spins by surface acoustic waves in undoped GaAs (110) quantum wells. TRKR measurements under an applied magnetic field demonstrate the coherent precession of the optically generated electron spin during acoustic transport over several micrometers and yield information about the relaxation processes for moving spins. © *2010 American Institute of Physics*. [doi:10.1063/1.3524218]

The moving piezoelectric potential Φ_{SAW} created by a surface acoustic wave (SAW) provides an efficient tool for the transport and manipulation of spins in semiconductor quantum wells (QWs).[1–3] These potentials can capture photogenerated electrons and holes in their spatially separated maxima and minima, respectively, thus dramatically increasing the recombination lifetime. The trapped carriers can then be transported with the well-defined SAW velocity v_{SAW} while maintaining the electron spin coherence over long distances. Long electron spin transport distances require the control of spin scattering mechanisms and, therefore, spin coherence time. The spatial separation of electrons and holes by the SAW field has the beneficial effect of reducing the electron-hole exchange interaction, which is a main spin scattering mechanism in undoped semiconductors [the Bir–Aronov–Pikus (BAP) spin dephasing mechanism].[1] A second important scattering mechanism for moving spins arises from the spin-orbit coupling [the Dyakonov–Perel (DP) spin dephasing[4]], which makes the spin precession angle dependent on the carrier trajectory. Two approaches have been proposed to reduce DP dephasing during acoustic transport in GaAs-based QW structures. The first consists of controlling the electron momentum and spin relaxation processes through mesoscopic confinement of carriers in moving potential dots produced by the interference of two SAW beams.[2] The second, which will be explored here, takes advantage of the special symmetry of GaAs (110) QWs. The latter makes DP spin dephasing processes inoperative for electron spins oriented along the growth axis, reducing also the overall dephasing of spins precessing around an axis lying in the QW plane.[3–8]

Previous investigations of the acoustically induced spin transport in (110) QWs were carried out using optical excitation to generate spin-polarized electron-hole pairs in an undoped QW. The spin density after transport was then detected by analyzing the circular polarization of the photoluminescence (PL) emitted when the carriers are brought to recombine after transport over several tens of micrometers.[2,3] The PL detection presupposes an efficient radiative recombination of the acoustically transported carriers, which is difficult to achieve in deep transport channels. In addition, the spin information is lost after recombination, thus limiting the use of this technique in many spintronics applications.

In this letter, we demonstrate an alternative approach to detect spins during acoustic transport in GaAs (110) QWs based on spatial- and time-resolved Kerr reflectometry (TRKR).[9,10] Here, the spins are optically generated using a circularly polarized pump laser pulse focused onto the SAW path (cf. inset of Fig. 1). They are then detected during acoustic transport by measuring the change in polarization of a weaker, linearly polarized probe pulse displaced by Δx and delayed by Δt with respect to the pump. An in-plane magnetic field perpendicular to the transport path induces the coherent precession of the spin vector as a function of Δx, thus delivering information about the spin scattering processes. This technique has also been recently successfully applied in spin relaxation studies in moving potential dots in GaAs QWs.[11]

The sample used in the studies consists of a 20 nm thick undoped GaAs (110) QW with $Al_{0.15}Ga_{0.85}As$ barriers located 400 nm below the surface. In order to enhance the piezoelectric field, the whole structure was coated with a 424 nm thick piezoelectric ZnO film. The SAW was generated along the $x \| [001]$ surface direction by an interdigital transducer (IDT) (cf. inset of Fig. 1) designed for an acoustic wavelength $\lambda_{SAW}=5.6$ μm. Attempts have been made to block the acoustic transport and induce the radiative recom-

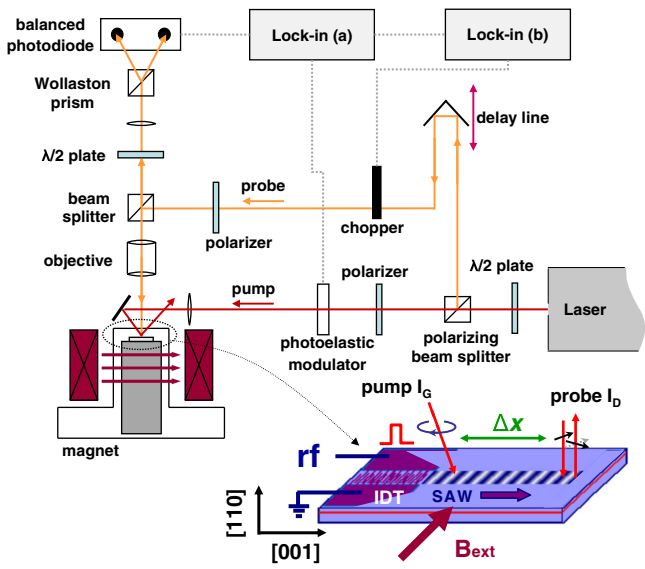

FIG. 1. (Color online) Setup for the detection of acoustic spin transport using TRKR. The IDT launches SAWs propagating along the [001] axis. Spin polarized electrons are excited by a circularly polarized pump beam and detected using a probe beam focused Δx away from the pump.

[a]Electronic mail: alberto@pdi-berlin.de.

bination of the carriers by depositing semitransparent metal stripes to short-circuit Φ_{SAW} at the surface.[2] Due to the sample geometry, however, the screening of Φ_{SAW} at the QW plane was not strong enough to induce a PL signal for spin detection.

The experiments were carried out with the sample in a microscope cryostat with an external coil to apply in-plane magnetic fields B_{ext} up to 0.15 T (Fig. 1). The output of a tunable Ti:sapphire laser producing 2 ps pulses with a repetition rate of 76 MHz is split into pump and probe beams which are focused at the generation (G) and detection (D) points with intensities I_G=100 μW and I_D=10 μW, respectively. The pump beam is polarization-modulated using a photoelastic modulator (PEM) operating at 50 kHz and focused under oblique incidence onto a 15 μm spot on the sample surface. The linearly polarized probe is focused onto a 10 μm spot and can be delayed by up to 5 ns relative to the pump using a 1 m delay line. The change in probe polarization induced by interactions with electron spins is detected by using a $\lambda/2$-plate, a Wollaston prism, and a pair of balanced photodetectors whose signal is detected by lock-in amplifiers synchronized with the PEM [lock-in (a)] and an optical chopper on the probe path [lock-in (b)].

The pulsed pump beam creates a high carrier concentration within the illuminated area of the undoped QW, which was probed by measuring the changes δI_R in the probe reflectivity as a function of position and time.[12] All measurements were carried out with the laser energy tuned to the electron heavy-hole exciton ($\lambda_{hh} \simeq 813.1$ nm), and using a SAW generated by applying P_{rf}=20 dBm to the IDT. In order to discriminate SAW effects from the thermal ones arising from the high P_{rf}, the rf and the laser excitations were applied in the form of square pulses at a frequency of ~200 Hz. The optical measurements were then carried out with the rf and optical pulses in-phase (SAW plus thermal effects) and out-of-phase (only thermal effects). Due to the slow thermal relaxation, the temperature is approximately the same in both cases. The latter was estimated to be approximately 53 K from the energetic shifts of the PL lines at the generation point.

The bright areas in the two-dimensional plot for δI_R in Fig. 2(a) show the spatial-temporal evolution of the carrier density generated by the pump beam under the acoustic field. The high carrier concentration around Δx=0 drifts initially slowly along the SAW propagation direction with an average velocity much smaller than the SAW velocity $v_{SAW}=\lambda_{SAW} f_{SAW}$=2.93 μm/ns (dashed line, where f_{SAW} =524 MHz is SAW resonance frequency at the measurement temperature). The low effective carrier velocity is attributed to the screening of the SAW piezoelectric field by the high carrier concentration present after the pump pulse. As a result, only a small fraction of the generated carriers are transported by each of the first SAW cycles following the pump. The carriers trapped in the first few SAW cycles lead to the faint cloud around the dashed line in Fig. 2(a). These carriers, however, maintain their spin polarization over long transport distances, as illustrated in Fig. 2(b), which displays the normalized TRKR signal δI_K for B_{ext}=65 mT detected under the same conditions as in Fig. 2(a). The clear oscillations in δI_K following the v_{SAW}-line are attributed to the precession of the photoexcited electron spins moving with v_{SAW} around the magnetic field B_{ext}.

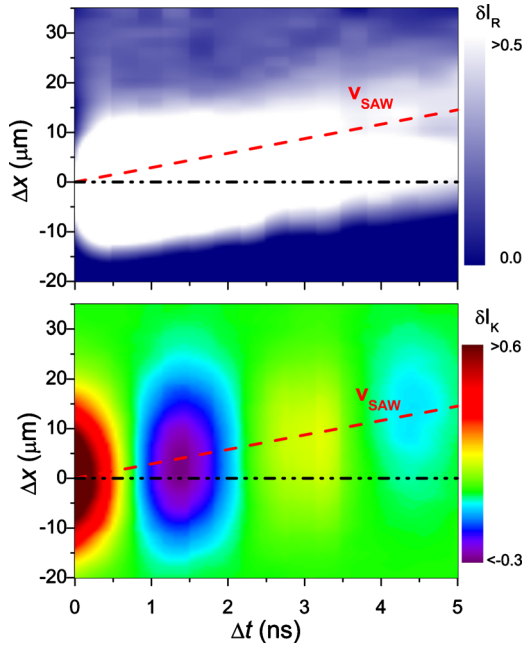

FIG. 2. (Color online) (a) Reflectivity (δI_R) and (b) Kerr signal (δI_K) as a function of the delay time (Δt) and distance (Δx) between pump and probe pulses under a magnetic field B_{ext}=65 mT and a SAW power P_{rf} =20 dBm. The dashed line has a slope equal to the SAW velocity v_{SAW}.

In order to extract quantitative information from the spatial-temporal plots (cf. Fig. 2), Fig. 3 displays profiles for δI_K recorded along the dashed (circles) and dot-dashed (squares) lines in Fig. 2(b), in the presence (open symbols) and absence (solid symbols) of a magnetic field B_{ext} =65 mT. The lines were obtained by fitting the measured data to the expected spin dynamics during Larmor precession under a transverse magnetic field B_{ext} given by

$$\delta I_K \propto \exp\left(-\frac{\Delta t}{T_2^*}\right)\cos(2\pi\nu_L\Delta t), \quad \nu_L = \frac{g\mu_B}{h}B_{ext}, \tag{1}$$

where g is the g-factor, μ_B the Bohr magneton, h the Planck's constant, ν_L the precession frequency, and T_2^* the

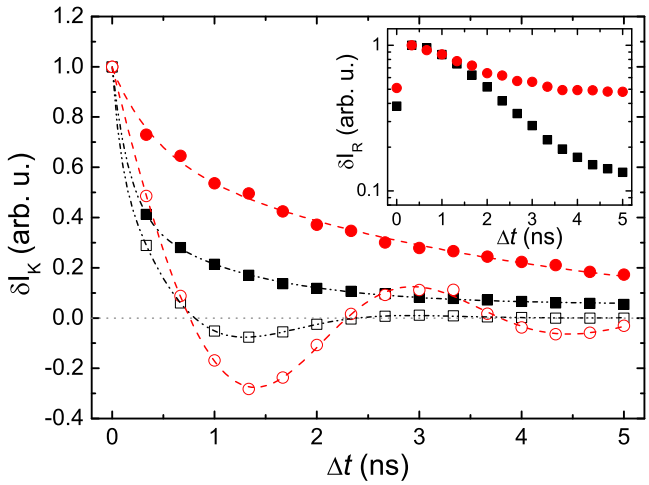

FIG. 3. (Color online) TRKR signal δI_K at Δx=0 in the absence of SAW (squares) and in the presence of a SAW [circles, measured along the dashed line in Fig. 2(b)]. The solid and open symbols were measured for B_{ext}=0 and 65 mT, respectively. The lines are fits of Eq. (1) to the data. The inset shows the corresponding time-resolved reflectivity δI_R obtained at Δx=0 without SAWs (squares) and along the SAW path [circles, from Fig. 2(a)].

effective relaxation time for precessing spins.[6] In our undoped samples, the intrinsic spin lifetime τ_s is related to T_2^* and to the carrier recombination time, τ_r, by the expression $\tau_s=(1/T_2^*-1/\tau_r)^{-1}$. τ_r was obtained from the time dependence of δI_R displayed in the inset of Fig. 3. Note, in particular, that τ_r enhances significantly under a SAW (filled cycles), reaching values close to 50 ns for $\Delta t>3$ ns.

All data sets for $B_{\text{ext}}=65$ mT can be fitted to Eq. (1) using a single precession frequency $\nu_L=(308\pm5)$ MHz, indicating that the contributions from the SAW field to the spin precession frequency[13] are negligible under the present experimental conditions. The g-factor $g\simeq0.35$ obtained from ν_L agrees well with reported values for electron spins in similar (110) QW samples.[3,6] This result is also consistent with a short hole spin relaxation time (in the tens of picosecond range), which makes the spin dynamics during acoustic transport entirely determined by the electron spins.

In contrast to ν_L, T_2^* and τ_r vary considerably among the different data sets in Fig. 3. We first consider the results obtained for $B_{\text{ext}}=0$ (filled symbols). The spin relaxation time $\tau_s=3.1\pm0.04$ ns measured in the absence of acoustic excitation (solid squares in Fig. 3) compares very well with those reported in Ref. 6 for $T\sim50$ K. The lifetime under these conditions is limited by BAP scattering induced by the high carrier density created by the pump pulse. The application of a SAW increases the lifetime to $\tau_s=4.1\pm0.3$ ns (solid circles), yielding spin transport lengths $v_{\text{SAW}}\tau_s>12$ μm. The latter is attributed to the reduction of BAP scattering as the electron-hole pairs are spatially separated by the SAW field. In fact, we have also observed that the SAW reduces by a factor of 20 the PL excited under conditions comparable to the one provided by the pump beam, thus attesting to a reduced electron-hole overlap despite the high carrier densities. The high excitation densities may, however, account for the shorter spin lifetimes as compared to the ones reported in Ref. 13.

Under a magnetic field, the lifetime of the electron spins becomes limited by the strong DP dephasing of their in-plane component, which appears when the electron momentum vector deviates from the [001] direction. In agreement with this expectation, the profiles with open symbols in Fig. 3 yield lifetimes $\tau_s=1.24\pm0.09$ ns (without a SAW) and $\tau_s=2.26\pm0.03$ (under a SAW), which are much shorter than those for $B_{\text{ext}}=0$

In conclusion, we have demonstrated that TRKR is a sensitive tool to probe the transport and manipulation of spins by SAWs as well as to study the limiting spin relaxation mechanisms.

We thank R. Farshchi for a discussion as well as M. Höricke, W. Seidel, and B. Drescher for the preparation of the samples. A. H.-M. thanks the support of the "Comissionat per a Universitats i Recerca del Departament d'Innovació, Universitats i Empresa de la Generalitat de Catalunya" and from the German DFG (priority program "semiconductor spintronics", Grant No. SPP1285).

[1]T. Sogawa, P. V. Santos, S. K. Zhang, S. Eshlaghi, A. D. Wieck, and K. H. Ploog, Phys. Rev. Lett. **87**, 276601 (2001).
[2]J. A. H. Stotz, R. Hey, P. V. Santos, and K. H. Ploog, Nature Mater. **4**, 585 (2005).
[3]O. D. D. Couto, Jr., F. Iikawa, J. Rudolph, R. Hey, and P. V. Santos, Phys. Rev. Lett. **98**, 036603 (2007).
[4]M. I. D'yakonov and V. Y. Kachorovskii, Sov. Phys. Semicond. **20**, 110 (1986).
[5]R. Eppenga and M. F. H. Shuurmans, Phys. Rev. B **37**, 10923 (1988).
[6]S. Döhrmann, D. Hägele, J. Rudolph, M. Bichler, D. Schuh, and M. Oestreich, Phys. Rev. Lett. **93**, 147405 (2004).
[7]O. Z. Karimov, G. H. John, R. T. Harley, W. H. Lau, M. E. Flatté, M. Henini, and R. Airey, Phys. Rev. Lett. **91**, 246601 (2003).
[8]Y. Ohno, R. Terauchi, T. Adachi, F. Matsukura, and H. Ohno, Phys. Rev. Lett. **83**, 4196 (1999).
[9]J. J. Baumberg, D. D. Awschalom, N. Samarth, H. Luo, and J. K. Furdyna, Phys. Rev. Lett. **72**, 717 (1994).
[10]R. T. Harley, O. Z. Karimov, and M. Henini, J. Phys. D: Appl. Phys. **36**, 2198 (2003).
[11]H. Sanada, T. Sogawa, H. Gotoh, K. Onomitsu, M. Kohda, J. Nitta, and P. V. Santos (unpublished).
[12]We verified that δI_R is proportional to the excitation densities (and, thus, to the carrier concentration) for time delays exceeding approximately 0.5 ns.
[13]O. D. D. Couto, Jr., R. Hey, and P. V. Santos, Phys. Rev. B **78**, 153305 (2008).